

# Resonant enhancement of magnetic damping driven by coherent acoustic phonons in thin Co<sub>2</sub>FeAl film epitaxied on GaAs

Lin Song<sup>1,2,‡</sup>, Wei Yan<sup>1,2,3,‡</sup>, Hailong Wang<sup>1,2</sup>, Jianhua Zhao<sup>1,2</sup>, and Xinhui Zhang<sup>1,2,†</sup>

<sup>1</sup>State Key Laboratory of Superlattices and Microstructures, Institute of Semiconductors, Chinese Academy of Sciences, Beijing 100083, China

<sup>2</sup>Center of Materials Science and Optoelectronics Engineering, University of Chinese Academy of Sciences, Beijing 100049, China

<sup>3</sup>Laser Institute, Qilu University of Technology (Shandong Academy of Sciences), Qingdao 266000, China

**Abstract:** The magnetic dynamics of a thin Co<sub>2</sub>FeAl film epitaxially grown on GaAs substrate was investigated using the time-resolved magneto-optical Kerr measurement under an out-of-plane external field. The intrinsic magnetic damping constant, which should do not vary with the external magnetic field, exhibits an abnormal huge increase when the precession frequency is tuned to be resonant with that of the coherent longitudinal acoustic phonon in the Co<sub>2</sub>FeAl/GaAs heterostructure. The experimental finding is suggested to result from the strong coherent energy transfer from spins to acoustic phonons via magnetoelastic effect under a resonant coupling condition, which leads to a huge energy dissipation of spins and a greatly enhanced magnetic damping in Co<sub>2</sub>FeAl. Our experimental findings provide an experimental evidence of spin pumping-like effect driven by propagating acoustic phonons via magnetoelastic effect, suggesting an alternative approach to the possible long-range spin manipulation via coherent acoustic waves.

**Key words:** magnetic damping; coherent longitudinal acoustic phonons; magnetoelastic effect; long-range spin manipulation

**Citation:** L Song, W Yan, H L Wang, J H Zhao, and X H Zhang, Resonant enhancement of magnetic damping driven by coherent acoustic phonons in thin Co<sub>2</sub>FeAl film epitaxied on GaAs[J]. *J. Semicond.*, 2021, 42(3), 032501. <http://doi.org/10.1088/1674-4926/42/3/032501>

## 1. Introduction

Magnetic dynamics of ferromagnet has been an active research field in the past few decades, aiming for the innovative design of low-power, high-speed, nonvolatile, and scalable spintronic devices<sup>[1, 2]</sup>. To this end, the half-metallic ferromagnets have received great attention in the field of spintronics for a complete spin polarization at the Fermi surface owing to its unique band structure<sup>[3]</sup>. In particular, as one of the widely studied half-metallic ferromagnets, Co-based Heusler alloys possess high spin polarization<sup>[4–6]</sup> and Curie temperature<sup>[7]</sup>, low damping factor<sup>[8, 9]</sup> and good lattice matching with traditional semiconductor GaAs substrate. These excellent characteristics make Co-based Heusler alloys ideal candidates as superior spin injection source in high-performance spintronic devices.

It is known that the magnetic damping governs the magnetization switching time of the magnetic recording device and determines the critical current density in the spin-torque-transfer devices<sup>[10, 11]</sup>. Therefore, it is of great significance to understand various physical mechanisms controlling the magnetic damping in ferromagnets. It has been demonstrated that several mechanisms can contribute to the magnetic damping. The intrinsic damping of a ferromagnet is governed by the spin-orbit coupling (SOC) and eddy-current mechanism<sup>[12–14]</sup>, while the extrinsic enhancement of damping

arises from the two-magnon scattering and magnetic inhomogeneous broadening, which are associated with the local defects and non-uniformity of magnetic thin films<sup>[15–17]</sup>. In the case of ferromagnet/nonmagnet bilayer structure, magnetic dynamics in the ferromagnetic layer can drive spin current into the adjacent nonmagnet and strongly influence the Gilbert damping of ferromagnet, which is known as spin pumping effect<sup>[18–20]</sup>. Moreover, the ferromagnetic resonance excitation by applying surface acoustic waves in a ferromagnet/normal-metal bilayer have been reported<sup>[21–24]</sup>, and spin current injection into the adjacent normal metal through magnetoelastic coupling were observed, demonstrating the spin pumping effect driven by the resonant coupling with coherent acoustic waves. Interestingly, recent studies have shown that spin angular momentum can be transferred to the acoustic phonons, which offers a great opportunity for long-range spin transfer and magnetic dynamics manipulation by coupling with the acoustic waves<sup>[25–29]</sup>. Such as the spin Seebeck effect, which was proved to result from a phonon-driven spin redistribution<sup>[25–28]</sup>. Spin transfer via the polarized phonons has also been proposed to be responsible for the long-range exchange coupling observed in a ferromagnet/semiconductor hybrid structure<sup>[29]</sup>. Recent theoretical investigation by Streib *et al.* showed magnetic dynamics manipulation by a phonon current that can inject spin angular momentum and energy into an adjacent nonmagnetic insulator, leading to an enhancement of damping in the ferromagnet<sup>[30]</sup>. This novel phenomenon is analogous to the spin pumping effect. Very recently, the remote magnetic dynamics coupling between two YIG films mediated by phonons in a thick GGG interlayer was experimentally observed<sup>[31]</sup>, and the long-range phonon-mediated

Lin Song and Wei Yan contributed equally to this work.

Correspondence to: X H Zhang, Email: [xinhuiz@semi.ac.cn](mailto:xinhuiz@semi.ac.cn)

Received 18 JANUARY 2021; Revised 10 FEBRUARY 2021.

©2021 Chinese Institute of Electronics

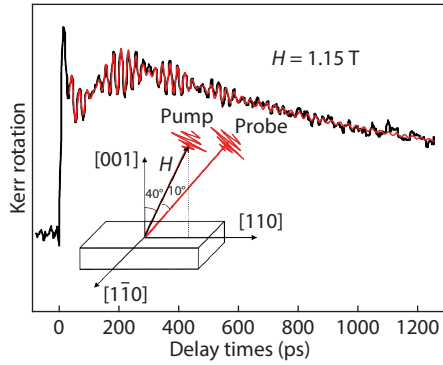


Fig. 1. TR-MOKE response for 3 nm-thick  $\text{Co}_2\text{FeAl}$  film with an external field of 1.15 T and its best fitting (red solid line). The inset shows the schematic diagram of application of external magnetic field.

spin transport in ferromagnet/nonmagnetic insulator bilayer was theoretically investigated as well<sup>[32]</sup>. These studies revealed promising route for phonon-mediated long-range spin transport, which is of great importance for spin manipulation and novel spintronic device design.

In this work, we investigated the ultrafast magnetization dynamics of  $\text{Co}_2\text{FeAl}$  thin film under an out-of-plane external magnetic field by using the time-resolved magneto-optical Kerr effect (TR-MOKE) technique. An abnormal huge increase in the intrinsic damping constant of a thin  $\text{Co}_2\text{FeAl}$  film was observed at the specific magnetic precession frequencies (or magnetic fields). And the respective precession frequencies were found to be resonant with the coherent acoustic phonons that were simultaneously generated in  $\text{Co}_2\text{FeAl}/\text{GaAs}$  heterostructure via magnetoelastic effect, with the help of further coherent acoustic phonon detection by the time-resolved pump-probe reflection measurements. The experimental findings demonstrate a strong coherent energy transfer from spins to acoustic phonons via magnetoelastic interaction under a resonant coupling condition, which is of great significance for future information technologies.

## 2. Experimental details

The  $\text{Co}_2\text{FeAl}$  thin films with different thickness were grown on the semi-insulating GaAs (001) substrate using molecular beam epitaxy (MBE) technique. A 150 nm-thick GaAs buffer layer was first grown before deposition of  $\text{Co}_2\text{FeAl}$  films, and a 2 nm-thick Al capping layer was deposited to prevent  $\text{Co}_2\text{FeAl}$  from oxidation. To study the coherent phonon excitation, a gold film with thickness less than 8 nm was evaporated on the chosen samples' surface by electron beam evaporation technique, since the gold film can serve as good heat sink to promote coherent acoustic phonon generation under the elastic distortion stress waves with intense optical excitation<sup>[33, 34]</sup>. Both the TR-MOKE measurements and transient reflection spectrum measurements were performed using a Ti:sapphire regenerative amplifier laser with the output pulse duration of 150 fs and repetition rate of 1 kHz at wavelength of 800 nm. For TR-MOKE measurements, the sample was mounted in an Oxford superconducting magnet with the out-of-plane magnetic field up to 3 T applied around  $40^\circ$  with respect to the normal direction [001] of  $\text{Co}_2\text{FeAl}$  film, as seen in the inset of Fig. 1. The in-plane projection of the external field was parallel to the [110] direction of the film, which is the easy axis of the cubic magnetic anisotropy. The pump

beam is directed onto the sample surface in the nearly same direction as the magnetic field and the probe beam is incident at an angle of  $50^\circ$  with respect to the surface normal. While for the transient reflection measurements taken with another pump-probe setup, the pump beam is at nearly normal incidence and the probe is incident at an angle of about  $30^\circ$  with respect to the surface normal without applying magnetic field, as seen in the inset of Fig. 3(a). All measurements were performed at room temperature.

## 3. Results and discussions

A thin  $\text{Co}_2\text{FeAl}$  film with a thickness of 3 nm was specifically employed for the magnetic dynamics study with TR-MOKE measurements. A typical TR-MOKE response measured at external field of 1.15 T for 3 nm-thick  $\text{Co}_2\text{FeAl}$  film is displayed in Fig. 1. It is noted that the dynamic response shows higher-frequency oscillations accompanied by a slowly oscillating envelope, indicating that there is more than one mode in the dynamic response, each with different frequency. With the help of fast Fourier transform (FFT) of the TR-MOKE data, the observed Kerr signal can be further fitted with

$$\Theta(t) = a + \sum_{i=1}^4 b_i \exp(-t/t_{0i}) + c_i \exp(-t/\tau_i) \sin(2\pi f_i t + \varphi_i), \quad (1)$$

where  $a$  and  $b_i$  are the background response magnitudes and  $t_{0i}$  is the recovery rate of magnetic anisotropy,  $c_i$ ,  $f_i$ ,  $\varphi_i$  and  $\tau_i$  are the amplitude, oscillation frequency, phase, and relaxation time of oscillating signal, respectively. The red solid line in Fig. 1 gives the best fit by Eq. (1) with four different frequencies, indicating that there exist four different modes for the Kerr response we observed.

The transient Kerr signals for 3 nm-thick  $\text{Co}_2\text{FeAl}$  film probed at different external magnetic fields are shown in Fig. 2(a). The extracted oscillatory frequency by Eq. (1) as a function of the external magnetic field is summarized in Fig. 2(b), a FFT spectrum of the TR-MOKE data measured at 1.6 T is also displayed in the inset as an example. One can immediately notice that, there is only one mode whose frequency increases almost linearly with the increased magnetic fields, while the frequencies of the other three modes remain constant, being 42.6, 32.3, and 19.6 GHz, respectively. The linearly-varying oscillatory frequency as a function of external field implies its magnetic excitation nature which can be described by the uniform magnetization precession with Landau-Lifshitz-Gilbert (LLG) phenomenological equation<sup>[35]</sup>:

$$2\pi f = \frac{\gamma}{\sin\theta_M} [H_1 H_2]^{\frac{1}{2}}, \quad (2)$$

where  $H_1 = \frac{2K_C}{M_S} \cos 4\theta_M - \frac{2K_U}{M_S} \cos 2\theta_M - 2 \left( 2\pi M_S - \frac{K_{\perp}}{M_S} \right) \cos 2\theta_M + H \cos(\theta_H - \theta_M)$ ,  $H_2 = \frac{2K_C}{M_S} \sin^4 \theta_M + \frac{2K_U}{M_S} \sin^2 \theta_M + H \sin \theta_M \sin \theta_H$ ,  $\gamma$  is the gyromagnetic ratio and  $M_S$  is the saturation magnetization;  $K_C$ ,  $K_U$ , and  $K_{\perp}$  are the in-plane cubic, uniaxial and out-of-plane magnetic anisotropy constants, respectively; and  $\theta_H$ ,  $\theta_M$  are the angles between the sample's normal and the directions of magnetic field and magnetization, respectively. With  $M_S = 1100 \text{ emu/cm}^3$  determined by the superconducting quantum interference device (SQUID) measurement, the red solid line in Fig. 2(b) shows the best fitting using Eq. (2), indic-

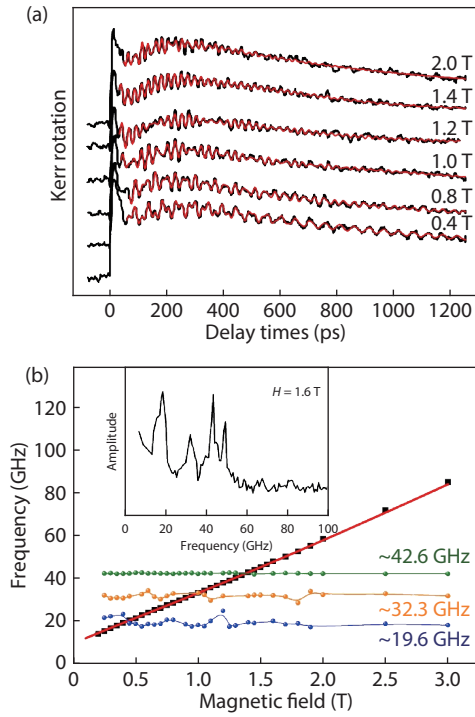


Fig. 2. For 3 nm-thick  $\text{Co}_2\text{FeAl}$  film, (a) TR-MOKE responses measured at different magnetic fields and their fittings (red solid lines), (b) the extracted oscillatory frequency as a function of external magnetic fields (the black squares represent the magnetization precession frequency and the red solid line is its best fitting; the colored dots represent the phonon modes whose frequencies do not depend on the magnetic fields). The inset in panel (b) shows the FFT spectrum of the TR-MOKE data measured at  $H = 1.6$  T.

ating the uniform magnetization precession response for the mode whose frequency varies linearly with the external magnetic field. The extracted fitting results for  $K_C$ ,  $K_U$ , and  $K_\perp$  are  $K_C = -7.86 \times 10^5$  erg/cm<sup>3</sup>,  $K_U = 2.926 \times 10^6$  erg/cm<sup>3</sup>,  $K_\perp = -4.68 \times 10^5$  erg/cm<sup>3</sup>, respectively. These values roughly agree with those obtained by rotating magneto-optical Kerr effect (ROT-MOKE) measurements in our previous studies<sup>[36, 37]</sup>. Here the much larger  $K_U$  than  $K_C$  with  $|K_U/K_C| = 3.7$  indicate the dominant uniaxial anisotropy for the investigated ultrathin thin 3 nm- $\text{Co}_2\text{FeAl}$  Film, and the nearly same value of  $|K_U/K_C| = 3.4$  was obtained in our previous ROT-MOKE measurements<sup>[36]</sup>.

While for the observed other three modes, it is noted that their frequencies did not vary with external magnetic fields, indicating that they are not associated with magnon excitation. But one can readily notice that the frequency of 42.6 GHz is consistent with that the well-known longitudinal acoustic (LA) phonon of GaAs<sup>[38, 39]</sup>. As for the other two low-frequency modes, our previous transient reflection studies for  $\text{Co}_2\text{MnAl}$  films with different thickness have revealed the similar phonon modes for the thicker  $\text{Co}_2\text{MnAl}$  films of 60 and 100 nm<sup>[40]</sup>. It is thus suspected that the three modes, whose oscillation frequencies are field-independent, should be associated with the coherent phonon excitation in  $\text{Co}_2\text{FeAl}/\text{GaAs}$  heterostructure. To clarify this, the time-resolved transient reflection experiments are further conducted<sup>[41, 42]</sup>.

The transient reflection first investigated for 3 nm- $\text{Co}_2\text{FeAl}/\text{GaAs}$  heterostructure is shown in Fig. 3(a), it con-

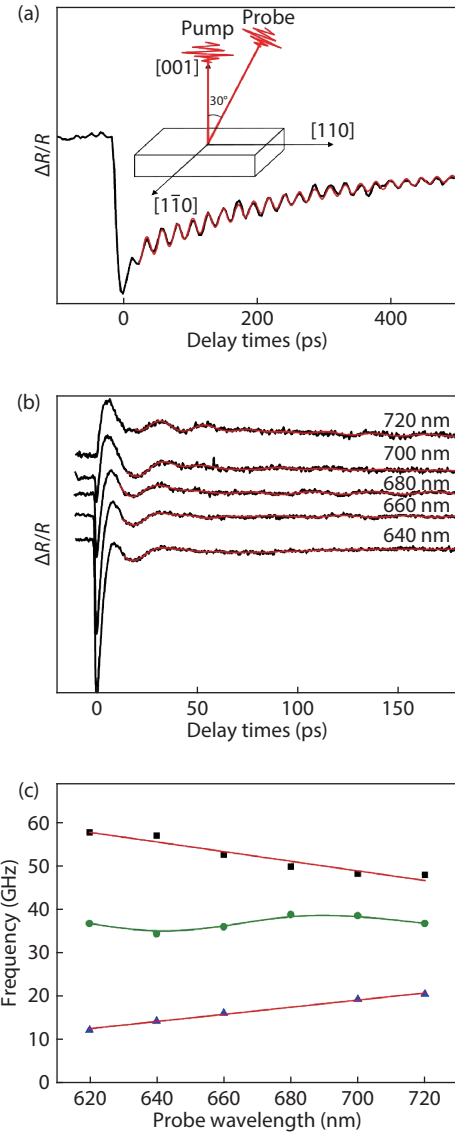


Fig. 3. The typical time-resolved reflection responses and their best fits (red solid line) for  $\text{Co}_2\text{FeAl}$  films with different thickness: (a) 3 nm- $\text{Co}_2\text{FeAl}$  measured at probe wavelength of 800 nm, (b) 45 nm- $\text{Co}_2\text{FeAl}$  measured at different probe wavelengths, (c) the extracted coherent acoustic phonon frequencies as a function of probe wavelength. The inset in panel (a) shows the schematic diagram of the experiment.

sists of two processes: one is the ultrafast electron dynamics reflecting the electron-phonon interaction at the initial time delay and the subsequent thermal relaxation with an exponential decay process; the other is the decaying periodic oscillation signal which is known to result from the interference between the probe pulse reflected from the surface and the probe pulse scattered at the propagating phonon pulses in the sample<sup>[42, 43]</sup>. The measured transient reflection responses can be fitted well by:

$$f(t) = a + b \exp(-t/t_0) + \sum_k c_k \exp(-t/\tau_k) \sin(2\pi f_k t + \varphi_k), \quad (3)$$

where the parameters  $a$ ,  $b$  and  $c_k$  are the fitting constants,  $t_0$  is the relaxation time of hot electrons,  $f_k$ ,  $\varphi_k$  and  $\tau_k$  correspond to the frequency, phase, and decay time of oscillation signals, respectively. The fitting results by Eq. (3) are shown as the red solid lines in Fig. 3(a). It is found that only the LA phon-

on mode of GaAs could be clearly observed for a 3 nm-thick  $\text{Co}_2\text{FeAl}$  film, the other two low-frequency modes are not observable within experimental sensitivity. The optically generated coherent LA phonon in GaAs for a thin 3 nm- $\text{Co}_2\text{FeAl}/\text{GaAs}$  heterostructure can be understood with the propagating strain pulse model<sup>[42]</sup>. In this model, the intense laser heating effect causes transient thermal expansion of crystal lattice and generates an ultrafast strain pulse, which propagates through the film and alters the local optical properties, so that the dielectric constant and refractive index can be changed. For the coherent detection of propagating acoustic waves, the probe pulse reflected from the top surface interferes with that partially reflected due to the discontinuity in the optical properties, and the coherent phonon frequency can be expressed as<sup>[42]</sup>:  $f = 2nv_s\cos\beta/\lambda_{\text{probe}}$ , where  $v_s$ ,  $n$  and  $\beta$  are the phonon velocity, refractive index and internal refraction angle of the sample, respectively. The velocity of the LA phonon at 43.11 GHz is calculated to be 4745 m/s, by taking the values of  $n = 3.67$ <sup>[44, 45]</sup> for GaAs at  $\lambda_{\text{probe}} = 800$  nm, and  $\beta \approx 8^\circ$  from Snell's law. This value is close to the known velocity of the longitudinal phonon mode reported in GaAs<sup>[46]</sup>.

As our previous work could detect the other two low-frequency modes in the thicker  $\text{Co}_2\text{MnAl}$  films<sup>[40]</sup>, we then prepared another thicker  $\text{Co}_2\text{FeAl}$  film (45 nm), its typical transient reflection signals probed at different wavelengths are presented in Fig. 3(b). The extracted frequencies as a function of probe wavelength are displayed in Fig. 3(c). It is seen that there are three phonon modes appearing in the transient reflection responses: two modes exhibit obvious dependence on the probe wavelength, but one mode at  $\sim 34$  GHz has negligible dependence on the probe wavelength. Note that these three phonon modes have also appeared in the TR-MOKE responses as shown in Fig. 2(b). It is noted that both the high- and low-frequency modes exhibit the same frequency dependent trend on the probe wavelength as we previously observed and discussed for  $\text{Co}_2\text{MnAl}$  films<sup>[40]</sup>. This indicates that the high-frequency mode originates from the coherent LA phonon generation in GaAs buffer, and the low-frequency mode should be associated with the coherent LA phonon generation in  $\text{Co}_2\text{FeAl}$  layer<sup>[38, 40]</sup>. Recall that the optical penetration depth at 800 nm for  $\text{Co}_2\text{FeAl}$  is only  $\sim 17.6$  nm<sup>[47]</sup>, the greatly attenuated pumping intensity passing through a thick  $\text{Co}_2\text{FeAl}$  (45 nm) layer will be too weak to optically excite coherent phonons in the underneath GaAs, thus the detected coherent phonon responses from a thick  $\text{Co}_2\text{FeAl}$  layer and its underneath GaAs buffer should mainly arise from the magnetoelastic coupling<sup>[48–53]</sup>. As for the mode with a frequency of  $\sim 34$  GHz, its negligible frequency dependence on the probe wavelength suggests that this mode may not be the coherent acoustic phonon response in  $\text{Co}_2\text{FeAl}/\text{GaAs}$  heterostructure. Instead, it may arise from the phonon echo which reflects back and forth from the upper and lower interfaces of a thin layer in the heterostructure<sup>[54]</sup>. According to echo frequency  $f_s = v_s/2d$ , the frequency arising from the phonon wave interference is evaluated to be  $\sim 35$  GHz, if taking  $v_s = 3850$  m/s obtained for  $\text{Co}_2\text{MnAl}$  films<sup>[40]</sup> and  $d = 55$  nm including the overall nominal thickness of Au, Al, and  $\text{Co}_2\text{FeAl}$  (45 nm) layers. But the phonon echo frequency for the 3 nm- $\text{Co}_2\text{FeAl}$  sample is estimated to be far from 32.3 GHz. The physical origin of the mode around 31–34 GHz is bey-

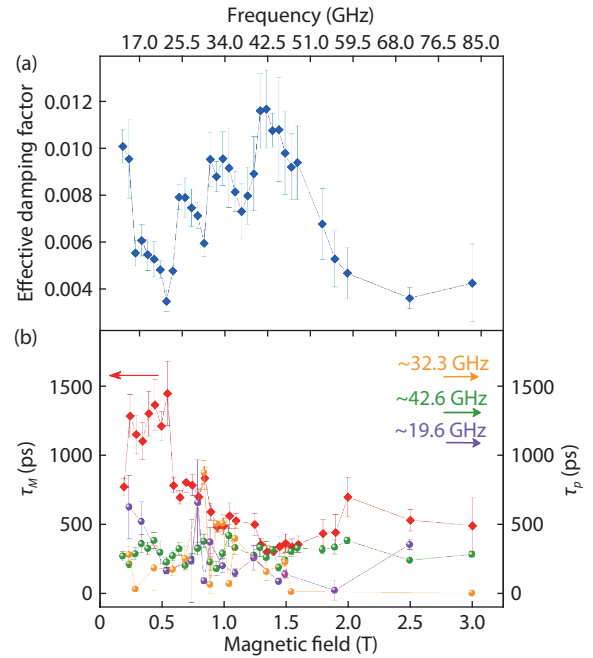


Fig. 4. For 3 nm-thick  $\text{Co}_2\text{FeAl}$  film: (a) the effective damping factors as a function of external magnetic fields, (b) the extracted magnetization relaxation time  $\tau_M$  and acoustic phonon decay time  $\tau_p$ .

ond our understanding and requires further study. Nevertheless, the transient reflection measurements have confirmed the coherent acoustic wave generation in  $\text{Co}_2\text{FeAl}/\text{GaAs}$  heterostructure. The impact of simultaneously generated coherent acoustic phonons on the magnetic damping of  $\text{Co}_2\text{FeAl}$  thin film is then revealed by further evaluating its damping factor as a function of magnetic fields.

By solving LLG equation, the Gilbert damping factor  $\alpha$  under the out-of-plane magnetic field can be determined from the following formula<sup>[35]</sup>:

$$\alpha = \frac{1}{\gamma\tau_M \left( H_1 + \frac{H_2}{\sin^2\theta_M} \right)}, \quad (4)$$

where  $H_1$  and  $H_2$  are defined the same as described in Eq. (2), and the magnetization relaxation time  $\tau_M$  can be obtained by fitting TR-MOKE response using Eq. (1). The extracted effective damping factor as a function of external magnetic fields by numerical fitting with Eq. (4) for the 3 nm-thick  $\text{Co}_2\text{FeAl}$  film is presented in Fig. 4(a). The remarkable feature in Fig. 4(a) is the abnormal huge increase of magnetic damping factor at the three specific fields (or precession frequencies) in the high-field regime where the damping factor is close to the intrinsic one, which should be independent of the external fields or precession frequencies as previously studied<sup>[16, 37, 55–57]</sup>. This is because that the inhomogeneous magnetic anisotropy distribution is greatly suppressed at sufficiently high fields ( $> 0.5$  T) and there is no extrinsic contribution from two-magnon scattering in the present case since the out-of-plane external field is applied about  $40^\circ$  from the normal direction of film<sup>[58, 59]</sup>. The greatly enhanced damping factor at low-field regime is known to result from the magnetic anisotropy inhomogeneous distribution<sup>[16, 37, 55–57]</sup>. The observed abnormal huge increase of intrinsic damping factor in the high-field regime is unexpected, with the large in-

crease ratio up to 119.7%, 161.9%, and 218.0% at 0.65, 1.0, and 1.35 T, respectively. However, it is noted that the abnormal increase of intrinsic damping factor appears at 0.65, 1.0, and 1.35 T, namely, at the precession frequencies of 25.3, 33.4, and 41.6 GHz, respectively. These specific precession frequencies are roughly in accordance with the three phonon frequencies observed in the transient reflection measurements as discussed above. This implies the huge enhancement of the damping factor when the magnetic precession of the film is in resonant with the coherent acoustic phonons. Fig. 4(b) presents the magnetization relaxation time  $\tau_M$  and acoustic phonon decay time  $\tau_p$  obtained by fitting TR-MOKE data using Eq. (1) for the 3 nm-thick Co<sub>2</sub>FeAl film. One can see that, unlike the huge abnormal increase of damping factor at the specific fields,  $\tau_p$  barely changes with the external fields, and  $\tau_M$  does not show apparent resonance decrease at the respective fields but exhibits a general decrease at high fields. As stated above, the inhomogeneous magnetization or field-dragging effect is supposed to be minimized at high fields comparing to that of low-field regime. The two-magnon scattering can be neglected with an out-of-plane external field applied about 40° from the normal of film. Hence the field-dragging effect or two-magnon scattering cannot be the primary cause of abnormal increase of damping factor observed at the specific fields.

Under an external out-of-plane magnetic field as in our experiment, it has been proved that the magnetization precession can be triggered by the longitudinal phonons in (Ga,Mn)As<sup>[60]</sup> and Ni films<sup>[61]</sup>. In these works, the magnetic anisotropy modification induced by the acoustic pulse-driven propagating strain can alter both the precession frequency and damping factor. This effect can be excluded in our all-optical excitation experiment since we only observed huge increase of damping factor, no precession frequency change was observed. In our experiment, an intense femtosecond laser pulse excites magnetic precession in Co<sub>2</sub>FeAl and coherent longitudinal phonons as well. As shown in Fig. 2(b), the three frequencies of 42.6, 32.3, and 19.6 GHz do not depend on the external fields, implying that they are not associated with the magnetic excitation. In addition, the magnetic precession frequency follows LLG equation quite well, showing no evident modulation by the phonon excitation. These facts indicate that the anomalous enhancement of magnetic damping in Co<sub>2</sub>FeAl is attributed to the resonantly enhanced coherent energy transfer from magnons to acoustic phonons, rather than from phonons to magnons. When the precession frequency is tuned with an external magnetic field to be resonant with the propagating coherent acoustic phonons in Co<sub>2</sub>FeAl/GaAs heterostructure, the coherent energy transfer from spins to acoustic phonons is greatly enhanced, leading to the enhanced damping of Co<sub>2</sub>FeAl owing to large energy dissipation. Note that the peak frequency around 25.3 GHz (0.65 T) in Fig. 4(a) showed a bit larger discrepancy with the measured acoustic phonon frequency around ~ 20 GHz. This could be caused by the broadened damping enhancement peak and rough tuning of external field around resonance. Since the resonant coupling would occur at the anticrossing regime of the magnon and phonon dispersion curves, which requires further theoretical calculation. As has been demonstrated previously, magnetoelastic waves can be excited through coherent energy transfer between optically excited

pure-elastic waves and spin waves via magnetoelastic coupling<sup>[62]</sup>. Our all-optical experimental finding suggested a huge spin energy loss and damping enhancement, analogue to a spin pumping effect, can be efficiently driven by resonant coupling between spin and coherent acoustic phonon excitations.

Recently, by utilizing ferromagnetic resonance (FMR) technique, An *et al.* have experimentally observed magnetic dynamics coupling between two YIG films over a macroscopic distance with a non-magnetic GGG spacer sandwiched in between<sup>[31]</sup>. The observed long-range magnetic dynamics coupling is attributed to the exchange interaction with the circularly-polarized coherent shear waves propagating in GGG dielectric, in which the transverse phonons carry the internal angular momentum<sup>[63–65]</sup>. With the coherent magnon-phonon coupling at interface<sup>[32]</sup>, the nonlocal spin current from one YIG film to the other YIG film can be efficiently mediated by the transverse phonons in GGG spacer, with a propagation length far exceeding that of magnon's by several orders of magnitude due to the low acoustic damping in these materials. In our work, the observed coherent acoustic phonons are discussed to be longitudinal phonons and they suppose do not carry angular momentum<sup>[66, 67]</sup>, so most likely there is no spin angular momentum transfer from spins to acoustic phonons. However, both the coherent energy and angular momentum transfer between spins and phonons would be expected if transverse acoustic phonon generation can be efficiently achieved, which would offer an alternative approach to long-range spin manipulation via acoustic phonons in ferromagnetic heterostructures.

#### 4. Conclusion

In conclusion, the magnetic damping of a thin Co<sub>2</sub>FeAl film is found to exhibit an abnormal huge increase at the precession frequencies that are resonant with that of the acoustic phonon excitations in the Co<sub>2</sub>FeAl/GaAs heterostructure. This finding is suggested to result from the enhanced coherent energy transfer from spin system to the propagating longitudinal acoustic phonons under a resonant coupling condition via magnetoelastic effect. This acoustic phonon-driven huge energy dissipation of spins leads to a greatly enhanced magnetic damping in Co<sub>2</sub>FeAl. Our work provides experimental evidence for potential long-range spin manipulation via propagating acoustic phonons in ferromagnetic heterostructures, which is of great significance for developing novel spintronic devices.

#### Acknowledgements

This work was supported by the National Key R&D Program of China (No. 2017YFB0405700), and National Natural Science Foundation of China (No. 12074370).

#### References

- [1] Žutić I, Fabian J, Sarma S D. Spintronics: Fundamentals and applications. *Rev Mod Phys*, 2004, 76, 323
- [2] Brataas A, Kent A D, Ohno H. Current-induced torques in magnetic materials. *Nat Mater*, 2012, 11, 372
- [3] de Groot R A, Mueller F M, van Engen P G, et al. New class of materials: Half-metallic ferromagnets. *Phys Rev Lett*, 1983, 50, 2024
- [4] Kübler J, Williams A R, Sommers C B. Formation and coupling of

- magnetic moments in Heusler alloys. *Phys Rev B*, 1983, 28, 1745
- [5] Ishida S, Fujii S, Kashiwagi S, et al. Search for Half-Metallic compounds in  $\text{Co}_2\text{MnZ}$  ( $Z = \text{IIIb, IVb, Vb}$  Element). *J Phys Soc Jpn*, 1995, 64, 2152
- [6] Picozzi S, Continenza A, Freeman A J.  $\text{Co}_2\text{MnX}$  ( $X = \text{Si, Ge, Sn}$ ) Heusler compounds: An ab initio study of their structural, electronic, and magnetic properties at zero and elevated pressure. *Phys Rev B*, 2002, 66, 094421
- [7] Webster P J. Magnetic and chemical order in Heusler alloys containing cobalt and manganese. *J Phys Chem Solids*, 1971, 32, 1221
- [8] Mizukami S, Watanabe D, Oogane M, et al. Low damping constant for  $\text{Co}_2\text{FeAl}$  Heusler alloy films and its correlation with density of states. *J Appl Phys*, 2009, 105, 07D306
- [9] Sukegawa H, Wen Z, Kondou K, et al. Spin-transfer switching in full-Heusler  $\text{Co}_2\text{FeAl}$ -based magnetic tunnel junctions. *Appl Phys Lett*, 2012, 100, 182403
- [10] Kikuchi R. On the minimum of magnetization reversal time. *J Appl Phys*, 1956, 27, 1352
- [11] Lee K, Kang S H. Development of embedded STT-MRAM for mobile system-on-chips. *IEEE Trans Magn*, 2011, 47, 131
- [12] Kamberský V. Spin-orbital Gilbert damping in common magnetic metals. *Phys Rev B*, 2007, 76, 134416
- [13] Hickey M C, Moodera J S. Origin of intrinsic Gilbert damping. *Phys Rev Lett*, 2009, 102, 137601
- [14] He P, Ma X, Zhang J W, et al. Quadratic scaling of intrinsic Gilbert damping with spin-orbital coupling in L10 FePdPt films: Experiments and Ab initio calculations. *Phys Rev Lett*, 2013, 110, 077203
- [15] Yuan H C, Nie S H, Ma T P, et al. Different temperature scaling of strain induced magneto-crystalline anisotropy and Gilbert damping in  $\text{Co}_2\text{FeAl}$  film epitaxied on GaAs. *Appl Phys Lett*, 2014, 105, 072413
- [16] Liu Y, Sheldford L R, Kruglyak V V, et al. Optically induced magnetization dynamics and variation of damping parameter in epitaxial  $\text{Co}_2\text{MnSi}$  Heusler alloy films. *Phys Rev B*, 2010, 81, 094402
- [17] Woltersdorf G, Heinrich B. Two-magnon scattering in a self-assembled nanoscale network of misfit dislocations. *Phys Rev B*, 2004, 69, 184417
- [18] Tserkovnyak Y, Brataas A, Bauer G E W. Enhanced Gilbert damping in thin ferromagnetic films. *Phys Rev Lett*, 2002, 88, 117601
- [19] Tserkovnyak Y, Brataas A, Bauer G E W. Spin pumping and magnetization dynamics metallic multilayers. *Phys Rev B*, 2002, 66, 224403
- [20] Fukuma Y, Wang L, Idzuchi H, et al. Giant enhancement of spin accumulation and long-distance spin precession in metallic lateral spin valves. *Nat Mater*, 2011, 10, 527
- [21] Weiler M, Dreher L, Heeg C, et al. Elastically driven ferromagnetic resonance in nickel thin films. *Phys Rev Lett*, 2011, 106, 117601
- [22] Weiler M, Huebl H, Goerg F S, et al. Spin pumping with coherent elastic waves. *Phys Rev Lett*, 2012, 108, 176601
- [23] Uchida K, An T, Kajiwara Y, et al. Surface-acoustic-wave-driven spin pumping in  $\text{Y}_3\text{Fe}_5\text{O}_{12}/\text{Pt}$  hybrid structure. *Appl Phys Lett*, 2011, 99, 212501
- [24] Li X, Labanowski D, Salahuddin S, et al. Spin wave generation by surface acoustic waves. *J Appl Phys*, 2010, 122, 043904
- [25] Uchida K, Adachi H, An T, et al. Long-range spin Seebeck effect and acoustic spin pumping. *Nat Mater*, 2011, 10, 737
- [26] Jaworski C M, Yang J, Mack S, et al. Spin-Seebeck effect: A phonon driven spin distribution. *Phys Rev Lett*, 2011, 106, 186601
- [27] Adachi H, Uchida K, Saitoh E, et al. Gigantic enhancement of spin Seebeck effect by phonon drag. *Appl Phys Lett*, 2010, 97, 252506
- [28] Uchida K, Xiao J, Adachi H, et al. Spin Seebeck insulator. *Nat Mater*, 2010, 9, 894
- [29] Korenev V L, Salewski M, Akimov I A, et al. Long-range p-d exchange interaction in a ferromagnet-semiconductor hybrid structure. *Nat Phys*, 2015, 12, 85
- [30] Streib S, Keshtgar H, Bauer G E W. Damping of magnetization dynamics by phonon pumping. *Phys Rev Lett*, 2018, 121, 027202
- [31] An K, Litvinenko A N, Kohn R, et al. Coherent long-range transfer of angular momentum between magnon Kittel modes by phonons. *Phys Rev B*, 2020, 101, 060407(R)
- [32] Ruckriegel A, Duine R A. Long-range phonon spin transport in ferromagnet/nonmagnetic insulator heterostructures. *Phys Rev Lett*, 2020, 124, 117201
- [33] Devos A, Côte R, Caruyer G, et al. A different way of performing picosecond ultrasonic measurements in thin transparent films based on laser-wavelength effects. *Appl Phys Lett*, 2005, 86, 211903
- [34] Liu W, Xie W, Guo W, et al. Coherent scattering of exciton polaritons and acoustic phonons in a ZnO single crystal. *Phys Rev B*, 2014, 89, 201201
- [35] Suhl H. Ferromagnetic resonance in Nickel ferrite between one and two kilomegacycles. *Phys Rev*, 1954, 97, 555
- [36] Qiao S, Nie S, Zhao J, et al. Temperature dependent magnetic anisotropy of epitaxial  $\text{Co}_2\text{FeAl}$  films grown on GaAs. *J Appl Phys*, 2015, 117, 093904
- [37] Qiao S, Nie S, Zhao J, et al. The thickness-dependent dynamic magnetic property of  $\text{Co}_2\text{FeAl}$  films grown by molecular beam epitaxy. *Appl Phys Lett*, 2014, 105, 172406
- [38] Miller J K, Qi J, Xu Y, et al. Near-bandgap wavelength dependence of long-lived traveling coherent longitudinal acoustic phonons in GaSb-GaAs heterostructures. *Phys Rev B*, 2006, 74, 113313
- [39] Matsuda O, Wright O B, Hurley D H, et al. Coherent shear phonon generation and detection with ultrashort optical pulses. *Phys Rev Lett*, 2004, 93, 095501
- [40] Yan W, Wang H, Zhao J, et al. Ultrafast optical probe of coherent acoustic phonons in  $\text{Co}_2\text{MnAl}$  Heusler film. *Chin Phys B*, 2017, 26, 016802
- [41] Thomsen C, Strait J, Vardeny Z, et al. Coherent phonon generation and detection by picosecond light pulses. *Phys Rev Lett*, 1984, 53, 989
- [42] Thomen C, Grahn H T, Marisetal H J, et al. Surface generation and detection of phonons by picosecond light pulses. *Phys Rev B*, 1986, 34, 4129
- [43] Lin H N, Stoner R J, Maris H J, et al. Phonon attenuation and velocity measurements in transparent materials by picosecond acoustic interferometry. *J Appl Phys*, 1991, 69, 3816
- [44] Aspnes D E, Kelso S M, Logan R A, et al. Optical properties of  $\text{Al}_x\text{Ga}_{1-x}\text{As}$ . *J Appl Phys*, 1986, 60, 754
- [45] Blakemore J S. Semiconducting and other major properties of gallium arsenide. *J Appl Phys*, 1982, 53, R123
- [46] Popović Z V, Spitzer J, Ruf T, et al. Folded acoustic phonons in GaAs/AlAs corrugated superlattices grown along the [311] direction. *Phys Rev B*, 1993, 48, 1659
- [47] Saito T, Matsuda O, Wright O B. Picosecond acoustic phonon pulse generation in nickel and chromium. *Phys Rev B*, 2003, 67, 205421
- [48] Chikazumi S. Physics of Ferromagnetism. New York: Oxford University Press, 1997
- [49] Bömmel H, Dransfield K. Excitation of hypersonic waves by ferromagnetic resonance. *Phys Rev Lett*, 1959, 3, 83
- [50] Schlomann E. Generation of phonons in high-power ferromagnetic resonance experiments. *J Appl Phys*, 1960, 31, 1647
- [51] Seavey M H. Microwave phonon generation by thin magnetic films. *IEEE Trans Ultrason Eng*, 1963, 10(1), 49
- [52] Ignatchenko V A, Kuzmin E V. Magnetoelastic interaction in a thin magnetic film. *J Appl Phys*, 1968, 39, 494
- [53] Seavey M H. Boundary-value problem for magnetoelastic waves in a metallic film. *Phys Rev*, 1968, 170, 560
- [54] Yamaguchi S, Tahara T. Coherent acoustic phonons in a thin gold film probed by femtosecond surface plasmon resonance. *J Ra-*

- man Spectrosc, 2008, 39, 1703
- [55] Liu Y, Shelford L R, Kruglyak V V, et al. Ultrafast optical modification of magnetic anisotropy and stimulated precession in an epitaxial  $\text{Co}_2\text{MnAl}$  thin film. *J Appl Phys*, 2007, 101, 09C106
- [56] Qiao S, Nie S, Zhao J, et al. Magnetic and Gilbert damping properties of L21- $\text{Co}_2\text{FeAl}$  film grown by molecular beam epitaxy. *Appl Phys Lett*, 2013, 103, 152402
- [57] Li T, Yan W, Zhang X, et al. Off-stoichiometry effect on magnetic damping in thin films of Heusler alloy  $\text{Co}_2\text{MnSi}$ . *Phys Rev B*, 2020, 101, 174410
- [58] McMichael R D, Stiles M D, Chen P J, et al. Ferromagnetic resonance linewidth in thin films coupled to NiO. *J Appl Phys*, 1998, 83, 7037
- [59] Landeros P, Arias R E, Mills D L. Two magnon scattering in ultrathin ferromagnets: The case where the magnetization is out of plane. *Phys Rev B*, 2008, 77, 214405
- [60] Scherbakov A V, Salasyuk A S, Akimov A V, et al. Coherent magnetization precession in ferromagnetic (Ga, Mn)As induced by picosecond acoustic pulses. *Phys Rev Lett*, 2010, 105, 117204
- [61] Kim J W, Vomir M, Bigot J Y. Ultrafast magnetoacoustics in nickel films. *Phys Rev Lett*, 2012, 109, 166601
- [62] Hashimoto Y, Bossini D, Johansen T H, et al. Frequency and wavenumber selective excitation of spin waves through coherent energy transfer from elastic waves. *Phys Rev B*, 2018, 97, 140404(R)
- [63] Garanin D A, Chudnovsky E M. Angular momentum in spin-phonon processes. *Phys Rev B*, 2015, 92, 024421
- [64] Holanda J, Maior D S, Azevodo A, et al. Detecting the phonon spin in magnonphonon conversion experiments. *Nat Phys*, 2018, 14, 500
- [65] Nakane J J, Kohno H. Angular momentum of phonons and its application to single-spin relaxation. *Phys Rev B*, 2018, 97, 174403
- [66] Tucker J W, Rampton V W. Microwave ultrasonics in solid state

physics. Amsterdam: North-Holland, 1972.

- [67] Kittel C. Interaction of spin waves and ultrasonic waves in ferromagnetic crystals. *Phys Rev*, 1958, 110, 836



**Lin Song** is currently a graduate student at the Institute of Semiconductors, Chinese Academy of Sciences. She received her B.S. degree of Applied Physics from Beijing University of Posts and Telecommunications in 2018. Her current interests focus on the ultrafast excitation of the collective spins and magnetization kinetics in the ferromagnet/semiconductor heterostructures.



**Xinhui Zhang** is a professor at the Institute of Semiconductors (IOS), Chinese Academy of Sciences (CAS). She received her B.S. and M.S. degrees from Shaanxi Normal University, in 1991 and 1994 respectively, and PhD degree from the Institute of Physics, CAS in 1997. From 1997 to 2005, she worked as postdoc and research associate at Lund University (Sweden); College of William and Mary (USA); The University of Oklahoma (USA); and University of Moncton (Canada), respectively. Since 2006, she worked as a professor at IOS, CAS. Her current research interests focus on the ultrafast spin dynamics in the low-dimensional semiconductors and ferromagnet/semiconductor heterostructures.